Static Properties Based Classification of Pneumatic Actuators - Potential of Progressive Effective Area Over the Stroke

Olivier Reinertz
RWTH Aachen University, Institute for Fluid Power Drives and Systems, Aachen, Germany
Olivier.reinertz@ifas.rwth-aachen.de

A variety of pneumatic actuator principles coexist on the market. The different designs are each dedicated to selected applications due to their specific properties and requirements. This paper aims to analyze the existing solutions by means of their static properties, to reveal innovation potential for new designs with enhanced operational behavior. It is based on a thorough investigation of the underlying physical correlations of force and stiffness. Thereof, a classification of existing principles is achieved, and a barely realized class of actuators with progressive effective area over the stroke is unveiled. A further analysis of the operational behavior of these actuators shows huge potential in selected applications. They are predicted to be superior in terms of performance and efficiency compared to existing solutions. A further analysis of the requirements on the design emphasizes the need for completely different realization concepts in comparison to the existing solutions. Finally, the paper closes by showing possible pathways to solve the actual challenges by incorporating new design methods.

DOI
https://doi.org/10.18690/um.fs.7.2025.9

ISBN
978-961-299-049-7

Keywords:
pneumatic,
actuators,
design,
actuator stiffness,
progressive force actuators

University of Maribor Press

1 Introduction

Pneumatic drives are widely used in mobile and industrial applications. While robustness and simple overload protection are key features of all fluid power actuators, open-loop controlled pneumatics additionally benefit from its simplicity in implementation and maintenance as well as low procurement costs. This makes technology especially relevant for automation tasks with low to medium power requirements. Other fields of application are mobile suspension systems and vibration isolating machine foundations, which benefit from the low stiffness of compressed air and the possibility of simple height adjustment during load changes. [1]

Different classes of pneumatic actuators can be distinguished by their design. The selection of a specific design for an application is usually driven by its robustness and geometric integratability. Furthermore, the curse of force and stiffness over the stroke and pressure and the friction induced hysteresis can be decisive parameters.

Usually, actuator sizing relies on the required stroke and the before-mentioned characteristics. Meanwhile, if standard control schemes are implemented to pneumatic drives, actuator sizing has a direct influence on the compressed air demand in operation. [2] Hence, the stroke and pressure dependent curse of force and stiffness of pneumatic actuators defines their sizing and directly influences the efficiency of the driven machines.

In the scope of this paper, the fundamental correlations of the static properties of pneumatic actuators are first deduced and then applied to the different actuator schemes on the market. Therewith, a new class of barely used actuators with progressive force over the stroke is unveiled and discussed by means of its usability in advantageous applications and its realizability. It will be shown that significant optimization in performance and efficiency is feasible by adapting the drive characteristics.

2 Fundamental static properties of pneumatic actuators

The fundamentals for calculating the main descriptive parameters for the operational behavior of pneumatic actuators, exerted force and stiffness, are briefly deduced in the following.

2.1 Fluidic force

For ideal actuators, which are free of friction and material hysteresis, a direct correlation between relative pressure(s), position, and the exerted fluidic force F_{fluid} exists. Hence, the force is independent from the fluid properties and the actuator's history.

The simplest load case for investigation of the actuator's force characteristic is the assumption of an incompressible fluid and an isobaric movement of the drive. Under these conditions the first law of thermodynamics can be easily applied. It requires that the fluidic energy provided to the actuator with volume V_A to hold its pressure p_{rel} constant during motion equals the mechanical work performed, which is given by the exerted force F_{fluid} and the stroke s in equation (1). This equation can be simplified to equation (2), which is generally applicable to all kinds of fluidic actuators.

$$p_{rel} \cdot \Delta V_A = p_{rel} \int_1^2 \frac{\partial V_A}{\partial s} ds = \int_1^2 F_{fluid}\, ds \tag{1}$$

$$F_{fluid} = p_{rel} \cdot \frac{\partial V_A}{\partial s} \tag{2}$$

It is obvious that the partial derivative of the volume over the stroke in the above-mentioned equation represents the fictitious active area of the actuator. Especially for non-linear systems, such as diaphragms, bellows and pneumatic muscles, this general relationship provides interesting insights into the actuator's fluid-mechanical properties, as will be shown in the following chapters. It should be noted that all forces, which result from the fluid pressure acting against the actuator chamber walls, which are transmitted through these walls or adjacent parts to the output, e.g., tensile forces in diaphragm walls, are included in the above calculation. Nevertheless, mechanical forces resulting from the mechanical stiffness of the actuator wall in the

working direction and/or friction forces at sliding seals need to be superimposed to the fluidic forces calculated with equation (2) for realistic results.

2.2 Actuator stiffness

The fluidic stiffness of an actuator can be expressed by the spring rate $k_{fluidic}$, which is defined by the local change in fluidic force F_{fluid} over the stroke with enclosed fluid. For a single actuator chamber, the fluidic stiffness results from equation (2) and is given by:

$$k_{fluidic} = -\frac{dF_{fluid}}{ds} = -\frac{dp_{rel}}{ds} \cdot \frac{\partial V_A}{\partial s} - p_{rel} \frac{d}{ds}\left(\frac{\partial V_A}{\partial s}\right) \tag{3}$$

Herein, the left term represents the portion of the actuator's stiffness, which results from a pressure change in the enclosed fluid due to the movement. Meanwhile, the right term covers stiffness, which results from a change in fictitious active area during displacement. Hence, the left term cannot be regarded without taking the compressibility of the enclosed fluid into account. To allow for fluid model integration, the change in fluid pressure needs to be a function of the fluid volume V_f, which equals the chamber volume V_A. Therefore, the equation is rearranged as follows:

$$k_{fluidic} = -\frac{dp_{rel}}{dV_f} \cdot \frac{dV_A}{ds} \cdot \frac{\partial V_A}{\partial s} - p_{rel} \frac{d}{ds}\left(\frac{\partial V_A}{\partial s}\right) \tag{4}$$

For soft actuators, the chamber volume changes not only with stroke but also with pressure. Therefore, partial derivatives of the volume with respect to the pressure and stroke need to be considered for a general stiffness equation:

$$dV_A = \frac{\partial V_A}{\partial s} ds + \frac{\partial V_A}{\partial p_{rel}} dp_{rel} = \frac{\partial V_A}{\partial s} ds + \frac{\partial V_A}{\partial p_{rel}} \cdot \frac{dp_{rel}}{dV_f} dV_A \tag{5}$$

Thereof, the volume change of the actuator over the stroke results:

$$\frac{dV_A}{ds} = \frac{\frac{\partial V_A}{\partial s}}{1 - \frac{\partial V_A}{\partial p_{rel}} \cdot \frac{dp_{rel}}{dV_f}} \tag{6}$$

The denominator of equation (6) shows that the pressure build-up in the fluid due to a reduction in volume and the wall strain caused by this pressure have an opposite effect on the stiffness. Stepping back to the right term of equation (4), the influence of the pressure on the partial derivative of the volume over the stroke needs to be considered for soft actuators. This leads to the following total derivative:

$$\frac{d}{ds}\left(\frac{\partial V_A}{\partial s}\right) = \frac{\partial^2 V_A}{\partial s^2} + \frac{\partial^2 V_A}{\partial s \partial p_{rel}} \cdot \frac{dp_{rel}}{ds} = \frac{\partial^2 V_A}{\partial s^2} + \frac{\partial^2 V_A}{\partial s \partial p_{rel}} \cdot \frac{dp_{rel}}{dV_f} \cdot \frac{dV_A}{ds} \tag{7}$$

Herein, the influence of the geometrical change in active area over the stroke is covered by the left term, while the right term describes the change in active area due to the stroke induced pressure fluctuation. Inserting equations (6) and (7) into equation (4) yields the general stiffness formulation for all kinds of actuators and arbitrary fluids:

$$k_{fluidic} = \frac{-\left(\frac{\partial V_A}{\partial s}\right)^2}{\frac{dV_f}{dp_{rel}} - \frac{\partial V_A}{\partial p_{rel}}} - p_{rel}\left(\frac{\partial^2 V_A}{\partial s^2} + \frac{\frac{\partial^2 V_A}{\partial s \partial p_{rel}} \cdot \frac{\partial V_A}{\partial s}}{\frac{dV_f}{dp_{rel}} - \frac{\partial V_A}{\partial p_{rel}}}\right) \tag{8}$$

A further assessment of the stiffness in pneumatic applications requires an approximation of the pressure/volume correlation of the gaseous fluid. Under the assumption that no change in air mass occurs during actuator motion, a polytropic change of state with the polytropic exponent n is used to describe the actuator's internal absolute pressure p_A:

$$p_A V_f^n = const. \quad \Rightarrow \quad \frac{dV_f}{dp_{rel}} = \frac{dV_f}{dp_A} = \frac{V_A}{-n \cdot p_A} \tag{9}$$

Under the assumption of a neglectable pressure-induced volume change and under consideration of the ambient pressure p_{amb} the stiffness calculates to:

$$k_{pneu} = \frac{n \cdot p_A}{V_A}\left(\frac{\partial V_A}{\partial s}\right)^2 - (p_A - p_{amb}) \cdot \frac{\partial^2 V_A}{\partial s^2} \tag{10}$$

The stroke dependent mechanical stiffness of the actuator housing, internal springs, etc. are neglected in the following, but can be superimposed to the result of the fluidic spring stiffness $k_{fluidic}$ or k_{pneu}. In the case of double acting drives, the stiffnesses of both chambers need to be considered.

3 Classification of existing pneumatic actuators

In the following, relevant existing design schemes of pneumatic actuators are described and classified according to the stroke dependence of their force. Therefore, positive stroke direction is chosen to raise the actuator's volume. Therewith all actuators move in positive direction during pressurization. To allow for better comparability, single acting devices are investigated. However, the results can be extrapolated to double-acting systems without any restrictions. For stiffness-evaluation of double acting devices, the stiffness of both chambers at the corresponding pressures needs to be taken into account.

3.1 Cylinders

The pneumatic cylinder is the primary actuator for automation purposes. Due to its rigid structure, volume increases linearly with the stroke and the differential in equation (2), which equals the fictitious active area, corresponds to the geometric piston area. Unavoidable seal friction needs to be considered and can pose a challenge in servo-controlled systems, low pressure applications or strongly miniaturized designs.

3.2 Membrane and diaphragm actuators

The sealing of the drive chamber by means of a flexible part allows to circumvent friction forces and leakages of translational seals of conventional cylinders. Depending on the shape of the used elastic part and piston, different designs with specific properties can be distinguished. The most relevant are briefly discussed in the following and depicted in Figure 1.

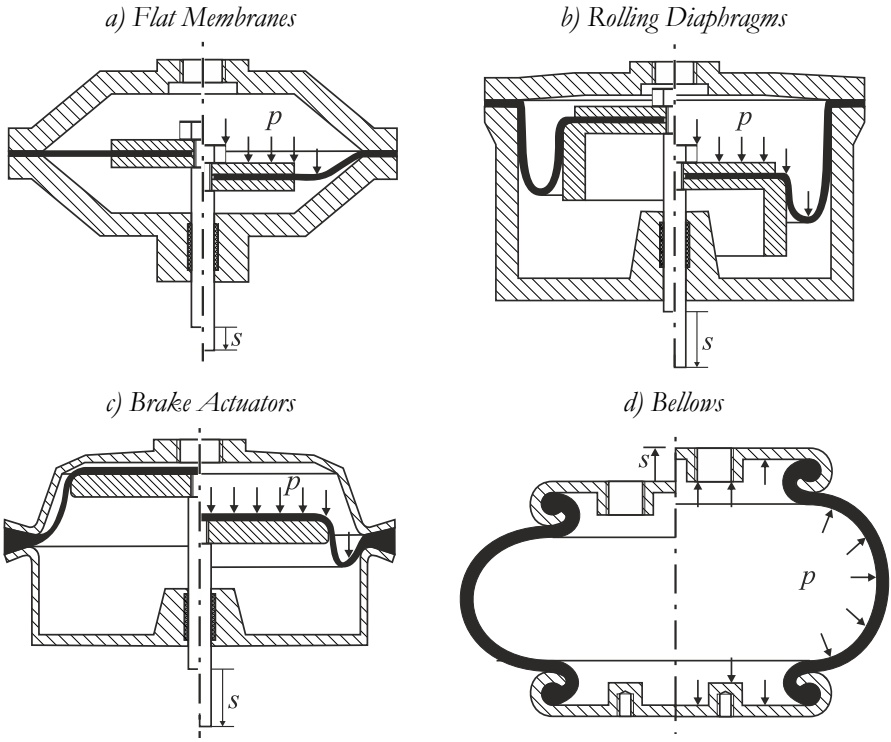

Figure 1: Investigated membrane actuators;
left: depressurized in neutral position, right: pressurized at stroke *s*;
Source: own

By using membranes or diaphragms for sealing, stick-slip effects at slow motion and hysteresis in force control can be avoided. This makes these actuators well suited as pneumatic springs in machine suspensions and actuators in control applications, e.g. for pneumatically controlled valves and brakes. Nevertheless, due to the viscoelastic material properties of the elastomeric parts used, some force hysteresis in cyclic motion is unavoidable [3].

3.2.1 Flat membranes

In Figure 1, a), a sketch of a typical realization of a flat membrane actuator is shown. To allow for sufficient mechanical stress distribution in the membrane, a rigid piston is connected to the load bearing rod, which holds the inner part of the membrane.

The membrane needs to allow for elastic deformation, as radial elongation is required for the piston stroke. Therefore, the stroke of flat membranes is usually very limited. If the piston moves out of its neutral position and pressure-induced deformation of the membrane is neglected, the membrane is deformed into a conical shape. Hence, the actuator's chamber volume can be described by the volume of a truncated cone, as given in equation (11). Herein the membrane geometry factor β equals the quotient of inner to outer diameter of the flexible part of the membrane and lies between zero and one.

$$\frac{\partial V_{dia}}{\partial s} = \frac{\pi R_{dia}^2}{3}(1 + \beta + \beta^2) \tag{11}$$

This equation obviously shows a stroke independent behavior, which is rarely achieved in real applications. Due to the elasticity of the membrane, the pressure leads to a convex shape of the membrane and therefore increases the chamber volume. According to *Yakovlev et al.* [4], the volume change of the drive chamber can be described by the semi-empirically deduced so called Liktan equation:

$$\frac{\partial V_{cyl}}{\partial s} = \frac{\pi R_{Cyl}^2}{3}\left(1 + \beta + \beta^2 - \frac{s}{\sqrt{5s_{max}(p)^2 - 5s^2}} \cdot (1 - \beta)\sqrt{4 + 7\beta + 4\beta^2}\right) \tag{12}$$

It is important to note that the design specific and pressure dependent imaginary stroke s_{max} cannot be reached by the actuator. The additional term of the Liktan equation is monotonically falling for constant pressure, which implies that the force of the actuator behaves accordingly.

3.2.2 Rolling diaphragm cylinders

The rolling diaphragm principle is widely used in applications requiring low friction and higher strokes compared to the flat membrane principle. The task of the rolling diaphragm is to seal the significant gap between piston and cylinder wall, as shown in Figure 1, b).

Therefore, it sticks on both the cylinder and the piston circumference and rolls from one surface to the other during piston motion. The rolling diaphragm is only pressurized from one side and its length in an axial cut plane stays constant over the

stroke. Hence, the bulge of the diaphragm curvature moves at half the piston speed. This leads to equation (13) for the description of the rolling diaphragm actuator's volume with cylinder wall radius R_{cyl} and piston radius R_{piston}. It is obvious that the actuator's force is, in analogy to a conventional cylinder, stroke independently. [5]

$$\frac{\partial V_{roll}}{\partial s} = \left(\frac{R_{cyl} + R_{piston}}{2}\right)^2 \cdot \pi \tag{13}$$

A drawback of this solution is, that the piston axial length, which directly influences the length of the actuator, needs to be at least half the stroke length. Therefore, rolling diaphragm actuators are suboptimal for higher stroke length especially in applications with strong demands on building space and weight.

In pneumatic suspension of mobile equipment, so called air bags are frequently used, which represent a special design of rolling diaphragms. The diaphragm is designed to withstand the tangential tensile forces generated by the pressurization, so that the outer support cylinder required for conventional rolling diaphragm devices can be omitted. A nearly constant force is achieved for isobaric conditions over the usual stroke regime. In the second stroke half, the exerted force usually decreases, as the diameter of the air bag decreases over its length to match the piston diameter at its end. Exemplary information on design and corresponding force characteristics can be found e.g. in [6].

3.2.3 Brake actuators

The demand for low costs, long lifetime, and reduced building space has led to the development of multiple designs of brake actuators, which differ among others in the shape of the membrane and piston. Besides rolling diaphragm designs there are also top hat membranes on the market [7]. A top-hat membrane is frequently used with a reduced piston length, ending up in a piston design being only a flat plate with rounded corners [8], as shown in Figure 1, c). Meanwhile, the diaphragm form stays comparable to a rolling diaphragm with the only difference in operating behavior, that a radial deformation of the diaphragm arises, which leads to additional chamber volume. As this chamber extension is very pronounced at stroke begin, the force in this regime is amplified. For symmetry reasons, the force reduces also at stroke end

accordingly, as the diaphragm is tensioned again by the axial piston movement and chamber volume increase is limited thereby. Mathematical description of the volume stroke correlation of such actuators is rather complex due to the pressure and stroke dependent deformation of the elastic diaphragm and the multiple geometry parameters, which need to be considered [9]. However, a rough approximation of the force can be achieved by using equation (12).

3.2.4 Bellows

Pneumatic bellows are primarily used in machine or vehicle suspension systems and as pneumatic actuators, if side and angular movements are unavoidable. They consist of two rigid plates, which are connected by one or multiple elastomeric bellows, as shown in Figure 1, d). The benefit of stacking multiple convolutions lies in the higher strokes feasible without excessive material deformation, while the total length to diameter ratio of such systems is limited by buckling effects. Therefore, the number of convolutions lies usually between one and three. [10]

The force characteristics have been investigated by *Quaglia and Guala* [11]. An exact analytical solution is not feasible, but good approximation is achieved by the following equation (14). Therein, the radius of the end plate R_{plate} and the longitudinal fixed length of the fiber reinforced elastic wall L_F define the actuator geometry and thus its force capability. The stroke is measured between the upper and lower end plate and is always smaller than the longitudinal wall length.

$$\frac{\partial V_{roll}}{\partial s} = R_{plate}^2 \cdot \pi \cdot \left(1 - \frac{L_F}{R_{plate}} \cdot \frac{\cos\left(a\sqrt{1-\frac{s}{L_F}}\right)}{a\sqrt{1-\frac{s}{L_F}}} \right) \quad \text{with} \quad a = \sqrt{\frac{\pi^3}{4\pi-8}} \tag{14}$$

The resulting equation describes a continuously decreasing force over the stroke at constant pressure.

3.3 Pneumatic artificial muscles

While common membrane and diaphragm actuators are built to push the load, pneumatic muscles are designed to pull the load during pressurization. Depending on the technical realization, different designs of pneumatic artificial muscles (PAMs) are distinguished. An overview is given in Figure 2.

These consist at least of two rigid end cups, which allow for their mechanical integration, and an interconnecting elastic wall. This wall contains or is wrapped by fibers that connect the two ends. The different designs differ in the geometry of the sealing wall and the arrangement of the fibers. The common working principle is that the radial pressure load on the elastic wall tends to raise the radius of the assembly. As the elasticity of the fibers is negligible, the distance of the end pieces must decrease as the radius increases while the pressure force on the end cups counteracts the fiber forces. As the surface of the end faces is usually very limited and the pressure force exerted by the elastic housing is amplified through the fiber arrangement, the fiber forces in axial direction are dominant and the device shortens during pressurization. In order to avoid the generation of torques at the end pieces, the fibers are usually symmetrically wound in both directions of rotation so that the resulting torques compensate for each other.

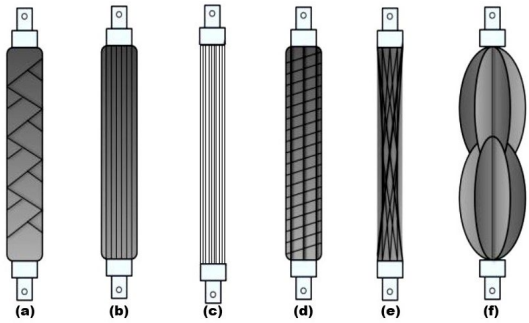

Figure 2: Overview of PAMs: (a) McKibben Muscle/Braided Muscle; (b) Pleated Muscle; (c) PAM reinforced by Kevlar Fiber; (d) Yarlott Netted Muscle; (e) Paynter Hyperboloid Muscle; (f) ROMAC Muscle;

Source: [11]

The only available design on the market is the McKibben PAM. According to *Takosoglu et al.* its static force/stroke characteristic can be modeled by equation (15) [13]. The parameters *b*, *n*, and *c* are positive numbers and need to be empirically adjusted by means of measurement data. For higher model accuracy these can be tuned as a function of the pressure.

$$\frac{\partial V_{PAM}}{\partial s} = R_i^2 \cdot \pi \cdot \left(b \cdot \left(1 - \left(\frac{s}{L_{max}}\right)^n\right) - c\right) \tag{15}$$

Thereof, it can be concluded that also for PAMs, which generate tensile forces, the force decreases over the stroke.

3.4 Summary of existing designs

The before-mentioned actuator designs and the stroke dependence of their force are summarized in Table 1. This overview demonstrates that actuators with stroke independent and decreasing force over the stroke exist. Actuators with continuously increasing force over the stroke at constant pressurization are non-existent on the market to date. The following chapter is dedicated to this non-existent class of actuators.

Table 1: Overview of existing designs

Actuator Design	Force characteristics	Force direction
Cylinder	stroke-independent	Single or double acting
Flat Membrane	mostly stroke-independent	Single or double acting
Rolling diaphragm	stroke-independent	Single acting
Brake actuator	mostly stroke-independent	Single or double acting
Bellow	Falling over the stroke	Only Extension
PAM	Falling over the stroke	Only Retraction

source: own

4 Actuators with increasing force over the stroke

The volumetric constraints to achieve actuators with significantly increasing force over the stroke at constant pressurization are achieved through differentiating equation (2), which leads to equation (16).

$$\frac{dF_{fluid}}{ds} > 0 \Rightarrow \frac{\partial^2 V_A}{\partial s^2} > 0 \tag{16}$$

It shows that the actuator volume needs to follow a progressively increasing function over the stroke. In the following, the potential of such actuators, their design challenges, which hinder their industrialization, and possible solutions are investigated.

4.1 Potential

Pneumatic actuators are widely used in many different applications with their own special demands on actuator performance. Therefore, in this chapter, only selected applications will be focused to highlight opportunities resulting from a progressive force/stroke characteristic.

4.1.1 Suspension systems

A closer look at the stiffness equations in chapter 2 unveils the potential to realize actuators, with outstanding stiffness properties. Therefore, at first, an actuator with parabolic volume stroke correlation, as given in equation (17), is investigated. Its force can be easily deduced, as shown in equation (18) Moreover, equation (10) is applicable and, due to its specific design, the resulting stiffness of the actuator in equation (19) is stroke independent.

$$V = \frac{A^2}{4B} + A \cdot s + B \cdot s^2 \tag{17}$$

$$F = (p_A - p_{amb}) \cdot (A + 2B \cdot s) \tag{18}$$

$$k = (2n - 1) \cdot 2B \cdot p_A + 2B \cdot p_{amb} \tag{19}$$

Another interesting application is to realize actuators, which allow for stiffness minimization while maintaining sufficient load bearing capability and small dead volumes. This is especially interesting for machine suspensions aiming to decouple the machine from the building structure by suspending the machine mass with the lowest possible eigenfrequency. A promising approach is an exponential volume/stroke characteristic, which results in the properties in equations (20) to (22).

$$V_{exp} = K \cdot \mathrm{e}^{(L \cdot s)} \tag{20}$$

$$F_{exp} = (p_A - p_{amb}) \cdot K \cdot L \cdot \mathrm{e}^{(L \cdot s)} \tag{21}$$

$$k_{exp} = ((n - 1) \cdot p_A + p_{amb}) \cdot K \cdot L^2 \cdot \mathrm{e}^{(L \cdot s)} \tag{22}$$

When comparing the operating behavior with the properties of a conventional actuator, e.g., a cylinder or a rolling diaphragm, a significant reduction in stiffness gets apparent. For comparison, the effective area A_{cyl} and position s_{cyl} of the cylinder can be determined in such a way that pressure, force, and volume are equal to the exponential actuator for a specific position s_0. This leads to the following equations:

$$F_{exp} = F_{cyl} = (p_A - p_{amb}) \cdot A_{cyl} \quad \Rightarrow \quad A_{cyl} = K \cdot L \cdot \mathrm{e}^{(L \cdot s_0)} \tag{23}$$

$$V_{exp} = V_{cyl} = s_{cyl} \cdot A_{cyl} \quad \Rightarrow \quad s_{cyl} = \frac{1}{L} \tag{24}$$

Thereof, the stiffness of the reference actuator in equation (25) results.

$$k_{cyl} = \frac{n \cdot p_A}{V_{cyl}} \left(\frac{\partial V_{cyl}}{\partial s_{cyl}} \right)^2 = n \cdot p_A \cdot K \cdot L^2 \cdot \mathrm{e}^{(L \cdot s_0)} \tag{25}$$

The comparison of equations (22) and (25) leads to equation (26). It demonstrates the strongly reduced stiffness in comparison to commonly used designs at significant chamber pressures for all polytropic coefficients between 1 and 1.4, as shown in in equation (27).

$$\frac{k_{exp}}{k_{cyl}} = \frac{n-1}{n} + \frac{p_{amb}}{n \cdot p_A} \tag{26}$$

$$\frac{p_{amb}}{p_A} < \frac{k_{exp}}{k_{cyl}} < 0.286 + 0.714 \cdot \frac{p_{amb}}{p_A} \tag{27}$$

Vice versa, a strongly reduced volume at the same stiffness in comparison to conventional actuators is achievable. Especially in the case of servo-controlled suspension systems, e.g. for position control or active damping, the volume reduction at constant stiffness can lead to significant improvements in control dynamics and compressed air demand.

4.1.2 Energy savings in automation

Compressed air consumption of pneumatic actuators with conventional control schemes, as e.g. downstream throttling or direct pressurization with the control-valve, is defined by the actuator chamber's volume at stroke end $V_A(s_{max})$, the specific

gas constant R and the pressure p_S and temperature T_S of the air supply, as shown in equation (28).

$$m_{Air} = \frac{p_S}{R \cdot T_S} \cdot V_A(s_{max}) \tag{28}$$

To fulfill the task, the actuator needs to overcome the force demand over the stroke $F_{Load}(s)$ in all positions, as shown in equation (29). Thereof, the minimum required compressed air mass to fulfill the task in equation (30) is achieved.

$$F_{Load}(s_A) < (p_S - p_{amb}) \cdot \frac{\partial V_A}{\partial s} \tag{29}$$

$$m_{Air,min} = \frac{p_S}{R \cdot T_S} \cdot \frac{\int_0^{s_{max}} F_{Load}(s_A) ds_A}{(p_S - p_{amb})} \tag{30}$$

If the application requires the highest force only at stroke end, which is the case in many clamping and pressing operations, the partial derivative of the volume over the stroke at stroke end needs to match the force demand. In the previous chapter, it has been shown that the volume change over the stroke of all existing actuators is either constant or decreases. This means, that in the entire stroke regime with lower force demand, strong oversizing of the actuator occurs. Therewith, for all existing actuators, the real air mass demand is given by equation (31).

$$m_{Air,conv} > \frac{p_S \cdot s_{max}}{R \cdot T_S} \cdot \frac{max\{F_{Laod}(s)\}}{(p_S - p_{amb})} \tag{31}$$

In contrast to this, if an exemplary drive with parabolic volume stroke correlation (see equation (17)) is used, which has only half of the maximum force at stroke begin and, in analogy to the before stated calculations, no dead volume, its stroke dependent volume and the resulting compressed air demand are given by equation (32) and (33). Thus, a 25 % reduction in air consumption is achieved simply by changing the actuator characteristic to a more application specific design.

$$V_{A,parab} = \frac{max\{F_{Laod}(s)\}}{2(p_S - p_{amb})} \cdot \left(s + \frac{s^2}{2s_{max}}\right) \tag{32}$$

$$m_{Air,parab} = \frac{3}{4} \frac{p_S \cdot s_{max}}{R \cdot T_S} \cdot \frac{max\{F_{Laod}(s)\}}{p_S - p_{amb}} \tag{33}$$

The optimization potential is application and actuator specific, as the load force needs to be overcome in all stroke positions and an actuator principle allowing for the optimal force/stroke correlation needs to be found.

4.2 Design challenges and solution approaches

The force of sliding-seal free actuators can be split into two parts: the stroke invariable pressure force, which acts directly on the movable rigid surface of the actuator chamber in direction of motion and the force contribution of the pressure forces acting against the actuator's wall and thus indirectly contributing to the actuator's force. The requirement of an increasing force over the stroke can therefore only be realized by changing the axial force of the side walls. It can be met either by a side wall, which decreasingly counteracts the pressure force on the moving end face over the stroke or by a side wall, which increasingly enforces the movement. In the following, due to the inherent reduction of the power density in the first case, only wall designs enforcing the actuator force are considered.

4.2.1 Tensile wall forces

Common nonlinear actuators possess elastic walls, which transmit primarily tensile forces on the moving end cap. The elasticity allows for a stroke variable cross-section of the actuator while the actuators' geometry is defined usually by integrated fibers with significant Young's modulus. To assist the drive's motion, these tensile forces need at least to act partially in moving direction. Theoretically, increasing assistance of these forces over the stroke can be achieved either by changing the forces' direction and/or its magnitude. Nevertheless, a design achieving the functionality mainly by changing the force direction has not been found to date. Instead, a change in assisting force magnitude can be achieved by the design proposed in Figure 3.

The main challenge in realization is to allow the pronounced tangential elongation of the elastic wall over the stroke without damage. A possible solution, which needs to be investigated in future, could be the use of a pumpkin inspired wall design in analogy to pleated muscles, with significantly higher stiffness in longitudinal compared to tangential direction.

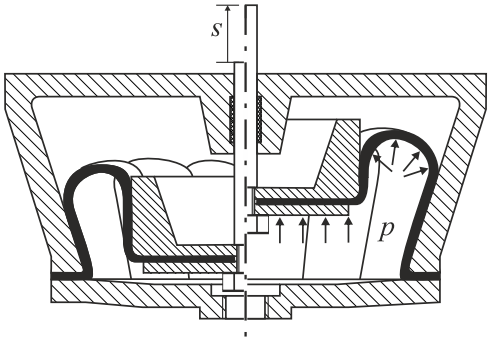

Figure 3: Rolling diaphragm in pumpkin inspired design
Source: own

4.2.2 Compressive wall forces

To allow for progressively increasing volume during elongation of the actuator a design with central constriction in analogy to an hourglass could be theoretically used, as it fulfills the volumetric requirements, see Figure 4, left. The constriction of the actuator shell is widened as the actuator elongates in axial direction. This leads to an additional volume increase over the stroke in comparison to conventional designs. However, the realization of such actuators would suffer from a compromise between rigidity of the wall for the compressive force transmission and elasticity of the wall for diameter and length change during motion. The same limitations apply to all elasticity-based design, if no additional rigid elements for force transmission are introduced.

A possible solution can be found by integrating rigid bars into the elastic wall of the hourglass design, which then represents a rotational hyperboloid, as shown in Figure 4, right. By allowing relative rotation of the two end caps, the central diameter increases at elongation of the actuator. Therewith, the elastic wall seals the system only between the rigid bars and is relieved from transmitting compressive forces. Unfortunately, strong angular distortions of the resulting facets between the rotating bars occur, which makes membrane design still a huge challenge.

An alternative to the above-mentioned designs is the introduction of an origami inspired actuator with rigid sealing facets, which are connected by sealed rotational joints. Despite the fact that such actuators cannot exist from a mathematical point

of view, as the bellows constriction prohibits the existence of a deformable polyhedron with a variable closed volume, the design in Figure 5 demonstrates that small deviations from a mathematically exact polyhedron by means of slight elasticity in selected segments (marked in blue in Figure 5) is sufficient for realization.

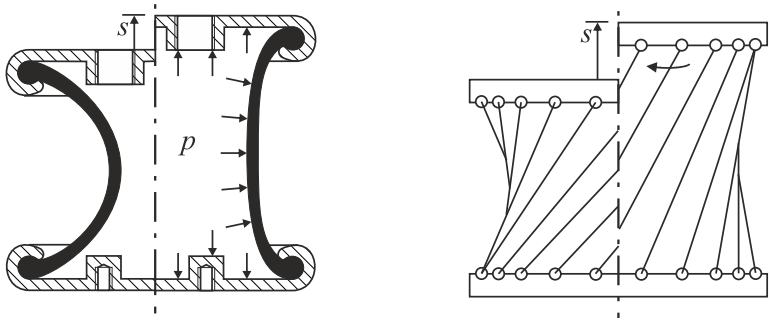

Figure 4: Hourglass actuator designs
Source: own

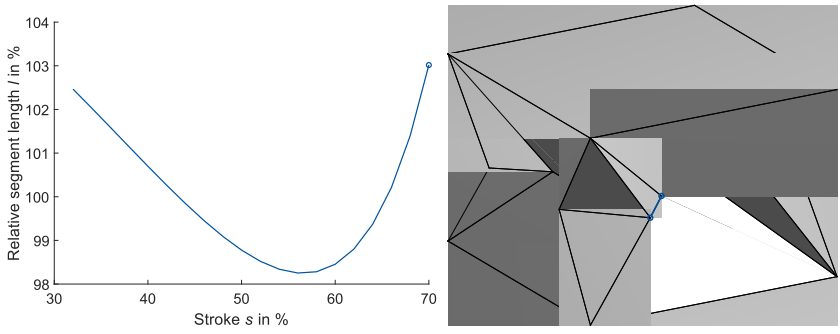

Figure 5: Origami inspired design and segment elongation during motion
Source: own

Obvious challenges are the implementation of the sealing system at all joints, the tolerance management to couple multiple facets to allow for a single degree of freedom in assembled state, the slight elasticity implementation and the fact, that a real actuator will have significant wall thickness to withstand internal pressure and compressive forces, which demands for significant design changes compared to the proposed principle.

5 Conclusion and Outlook

In the scope of this paper, a generalized form of the force and stiffness calculation for pneumatic actuators, which bases solely on the description of their internal volume in operation has been deduced. These fundamentals are not only relevant for the description of conventional pneumatic drives but can also enable fluidic stiffness calculation of soft actuators in early design stages by means of model-based calculation of the volume under deformation and pressurization.

Furthermore, these equations enable the classification of all relevant existing solutions of industrial pneumatic drives by their static characteristics. The result shows a whole class of actuators with progressive effective area over the stroke, which are neither available on the market nor systematically researched.

A first investigation of the potential of such actuators unveils different applications – clamping, pressing and machine suspension – that can be significantly optimized by replacing conventional actuators with devices of this new class. Consequently, the main arising design challenges are investigated and possible solutions discussed. Three different promising designs were elaborated, the conical rolling diaphragm in pumpkin design, the rotational hyperboloid actuator with push bars and the origami inspired actuator. Further studies on the realizability, arising challenges and the measured operational behavior of prototypical realizations are aspired in future.

References

[1] Murrenhoff, H., Reinertz, O.: *Fundamentals of Fluid Power - Part 2: Pneumatics*, 2nd edition, Shaker, Aachen, Germany, ISBN: 978-3-8440-3213-0

[2] Doll, M., Neumann, R., Sawodny, O.: *Dimensioning of pneumatic cylinders for motion tasks*, International Journal of Fluid Power, 2015, 16(1), pp. 11–24, doi: 10.1080/14399776.2015.1012437

[3] Gong, Y., Guo, H.: *Measurement and Modeling of Hysteresis in Pneumatic Actuator Under Different Loading Rate*, Proceedings of China SAE Congress 2018: Selected Papers, Lecture Notes in Electrical Engineering 574, Springer Nature Singapore, 2020, doi: 10.1007/978-981-13-9718-9_4

[4] Yakovlev et al.: *Static Characteristic of a Membrane Pneumatic Actuator*, Russian Engineering Research, 2022, 42(4), pp. 391–394, doi: 10.3103/S1068798X22040323

[5] N.N.: *Diaphragm Design Guidebook*, DiaCom Corporation, 2018

[6] N.N.: *Axle Guide – Running Gears for Commercial Vehicles: Selection, Design, Installation*, 1st edition, BPW Bergische Achsen KG, 2023

[7] N.N.: *Spring Brake Actuators for Air Disc Brakes*, Service Manual, Rev. 001, Knorr-Bremse Systeme für Nutzfahrzeuge GmbH, 2015
[8] Moni, Arangarason, A.: *Brake Chamber Type 12*, Specification Drawing, WABCO, 2021
[9] Fojtášek, K., Dvořák, L.: *Mathematical Modeling of Diaphragm Pneumatic Motors*, EPJ Web of Conferences, 2014, doi: 10.1051/epjconf/20146702028
[10] Chen, J.-J., et al.: *Theoretical modelling and experimental analysis of the vertical stiffness of a convoluted air spring including the effect of the stiffness of the bellows*, Proceedings of the Institution of Mechanical Engineers, Part D: Journal of Automobile Engineering, 2018, Vol. 232(4), pp. 547–561, doi: 10.1177/0954407017704589
[11] Quaglia, G., Guala, A.: *Evaluation and Validation of an Air Spring Analytical Model*, International Journal of Fluid Power, 2003, 4(2), pp. 43-54
[12] Kalita, B., Leonessa, A., Dwivedy, S. K.: *A Review on the Development of Pneumatic Artificial Muscle Actuators: Force Model and Application*, Actuators, 2022, 11, 288, doi: 10.3390/act11100288
[13] Takosoglu, J. E. et al.: *Determining the Static Characteristics of Pneumatic Muscles*, Measurement and Control, 2016, 49(2), doi: 10.1177/0020294016629176